

Circumnuclear star formation in the barred galaxy NGC 1022

J. A. García-Barreto^{1,2}, D. Downes³, F. Combes^{4,5}, L. Carrasco⁶, M. Gerin^{4,5}, and I. Cruz-Gonzalez²

¹ Max Planck Institut für Radioastronomie, Auf dem Hügel 69, W-5300 Bonn 1, Federal Republic of Germany

² Instituto de Astronomía, Universidad Nacional Autónoma de México, Apartado Postal No. 70-264, México D.F., 04510 México

³ Institut de Radio Astronomie Millimétrique, Domaine Universitaire, F-38406 St. Martin d'Hères, France

⁴ DEMIRM, Observatoire de Meudon, F-92195 Meudon, France

⁵ Radioastronomie Millimétrique, ENS, 24 Rue Lhomond, F-75231 Paris, France

⁶ Observatorio Astronómico Nacional, IA-Universidad Nacional Autónoma de México, Apdo. Postal 877, Ensenada, Baja California, C.P. 22830, México

Received April 19, accepted June 3, 1991

Abstract. Observations of ring like structures around the compact nucleus of a bar galaxy are useful for determining whether the structure is at the expected location of a resonance and also whether there is star formation in them. We observed the barred spiral galaxy NGC 1022 in the radio continuum at 20, 6, and 2 cm, in CO(1–0) and CO(2–1) and in the near infrared J , H and K bands. No evidence was found for a circumnuclear ring like structure either from our radio continuum or our CO observations. Radio continuum emission is only detected from the central 20" of the galaxy, in a compact core and a weaker second component to the north. The spectral indices of the integrated fluxes at the three wavelengths are flatter than an average disk spectral index, $\alpha_{\text{disk}} \simeq -0.75$, namely $\alpha_{20}^6 = -0.52$, $\alpha_{20}^2 = -0.23$ and $\alpha_6^2 = -0.03$. From our millimeter observations we estimate a molecular hydrogen mass within a diameter of 3.3 kpc of $1 \cdot 10^9 M_{\odot}$. The observed near-infrared colors are $J-H = 0.82$ and $H-K = 0.35$. From our observations with an aperture of 14", together with smaller aperture observations by Devereux et al. we estimate a mass within 200 pc of $2 \cdot 10^9 M_{\odot}$.

Key words: galaxies: barred – galaxies: individual: NGC 1022 – galaxies: nuclei of – radio continuum – star formation

$\log[f(12)/f(25)] \simeq -0.62$ similar to other galaxies with central star formation activity; its near infrared colors are somewhat redder than the colors of normal spiral galaxies $J-H = -0.82$, $H-K = 0.35$; and its dust temperature, assuming $S_{\nu} \simeq \nu B_{\nu}(T)$, is 40 K.

NGC 1022 is a barred spiral classified as SBa(r)p with an optical diameter of $\sim 150''$, at an inclination of between 24° and 28° (Grosbol 1985; Tully 1988) and is located in the Cetus-Aries Cloud of galaxies, Tully's (1988) group 52-1, at a distance of 15 Mpc (for $H_0 = 100 \text{ km s}^{-1} \text{ Mpc}^{-1}$). Previous observations of NGC 1022 include multi-aperture UBV photometry of the central region (Griessmith 1980); large aperture $H\alpha$ (Kennicutt & Kent 1983); multi-aperture H (1.65 μm) and K (2.2 μm) fluxes from the central region (Devereux 1989); 10 μm emission from the nuclear region (Devereux 1987); H I observations (Fisher & Tully 1981; Huchtmeier 1982); low resolution observations of CO(1–0) (Solomon & Sage 1988); low resolution radio continuum observations at 18 cm and 21 cm (Norris et al. 1989) and at 20 cm (Puxley et al. 1988).

In this paper we describe new radio continuum observations at 20, 6 and 2 cm with low and high angular resolution, new near-infrared photometry from the central 14" region and new CO(1–0) and CO(2–1) observations.

1. Introduction

IRAS observations of spiral galaxies have indicated that galaxies with a bar have FIR colors characteristic of star formation activity in the vicinity of the compact nucleus (Hawarden et al. 1986). In some cases, the detection of radio continuum emission, $H\alpha$, 10 μm and sometimes CO emission support this scenario. Numerical simulations on the other hand have predicted the formation of ring like structures at the locations of inner and outer Lindblad resonances (Schwartz 1981, 1984; Combes & Gerin 1985; Combes 1988). We have selected NGC 1022 in order to make new observations of its radio continuum and CO emissions and new JHK photometry observations with an aperture of 14". NGC 1022 has FIR colors $\log[f(60)/f(100)] \simeq 0.12$ and

2. Radio continuum observations and results

We observed NGC 1022 with the VLA with low resolution at a wavelength of 20 cm in 1988 and with high resolution at 20, 6 and 2 cm in 1989. The high resolution observations were made at 20 cm in the A/B array, at 6 cm in the B/C array and at 2 cm in the C/D array, to have similar uv coverage at each frequency. Table 1 gives the observing parameters. The data from circular polarizations in two 50 MHz passbands were combined and cleaned to give total intensity maps at 1.49, at 4.86 and at 14.94 GHz. The low resolution D -array observation at 20 cm yielded the total flux and extent of the radio continuum emission.

Our low resolution map at 20 cm (Fig. 1) shows an unresolved source, with a peak flux density of 43.4 mJy, coincident with the galaxy in agreement with a previous 21 cm flux determination of $\leq 48 \text{ mJy}$ (Norris et al. 1989). Three background sources were detected in the field (Table 2). No extended emission was detected

Send offprint requests to: J. A. García-Barreto (Mexican address)

Table 1. Observational parameters for NGC 1022

<i>Radio continuum:</i>				
Frequency	1.4 GHz	1.4 GHz	4.8 GHz	14.9 GHz
VLA array	<i>D</i>	<i>A/B</i>	<i>B/C</i>	<i>C/D</i>
Date of observation	Sep. 1988	Feb. 1989	May 1989	Oct. 1989
Amplitude calibrator	3 C48	3 C48	3 C48	3 C48
Flux amplitude calibrator	15.76 Jy	15.76 Jy	5.57 Jy	3.45 Jy
Bandwidth	100 MHz	100 MHz	100 MHz	100 MHz
Phase calibrator	0237-233	0237-233	0237-233	0237-233
r.m.s.	1.5 mJy/beam ⁻¹	0.065 mJy beam ⁻¹	0.06 mJy beam ⁻¹	0.24 mJy beam ⁻¹
HPBW	42" × 34"	3'47 × 1'47	3'62 × 1'49	3'9 × 1'66
<i>CO:</i>				
Transition	1–0	2–1		
Frequency	115.271 GHz	230.538 GHz		
HPBW	44"	22"		
Heliocentric velocity	1460 km s ⁻¹	1460 km s ⁻¹		
Half power linewidth	120 km s ⁻¹	120 km s ⁻¹		
Peak line temperature, <i>T</i> _{mb}	0.15 K	0.28 K		

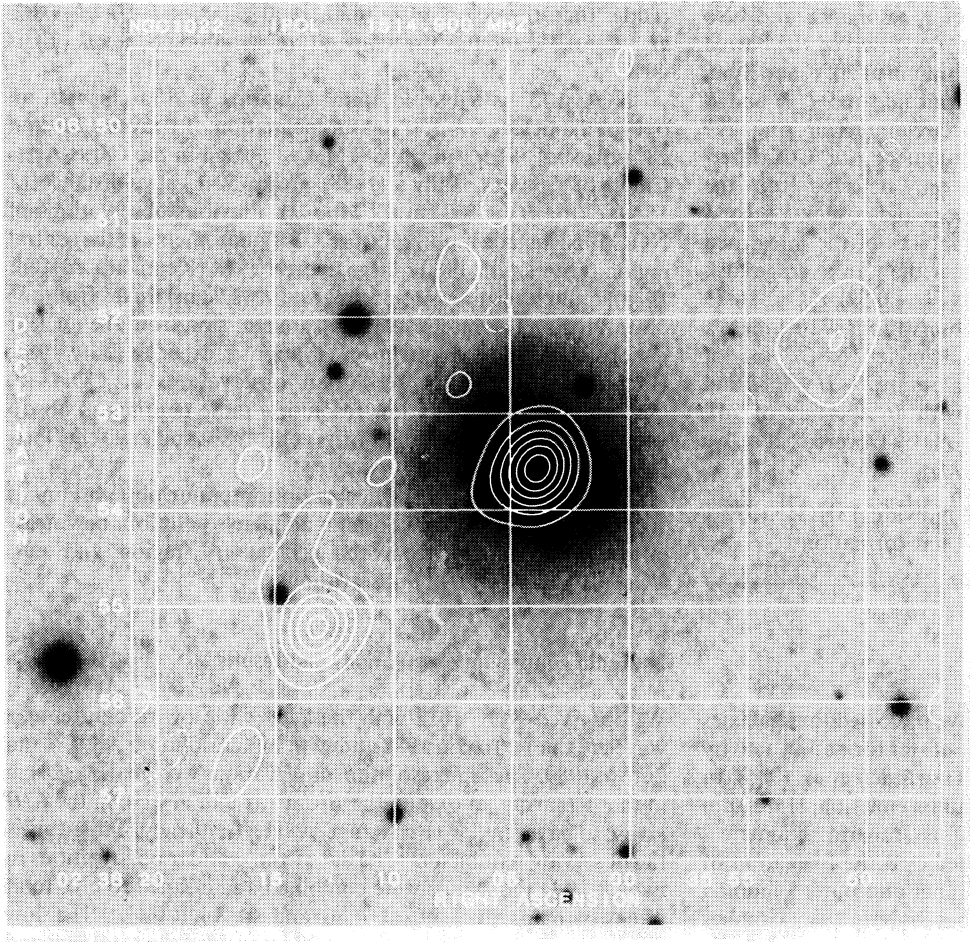


Fig. 1. Low resolution radio continuum emission at 20 cm from NGC 1022 superposed on a POSS blue sensitive print. The contours are -3.5 , 3.5 , 10.5 , 17.5 , 24.5 , 31.5 , and 38.5 mJy beam⁻¹

Table 2. Background sources in the field of NGC 1022

Source	Right ascension (1950.0)	Declination (1950.0)	20 cm peak flux D^a (mJy)
1	02 ^h 36 ^m 13 ^s .19	−06°55′13″.3	34
2	02 ^h 35 ^m 51 ^s .20	−06°52′16″.1	11
3	02 ^h 35 ^m 44 ^s .58	−06°41′51″.7	96

^a No attempt has been made to correct for primary beam dilution.

from NGC 1022 outside the central 60'' to a level of 1.5 mJy beam^{−1}.

We made high resolution maps with the full uv coverage at the three wavelengths using a restoring beam of 3''.9 × 1''.7 (Fig. 2). Figure 3 shows the high resolution 6 cm map superimposed on a POSS blue sensitive photograph. The angular resolution in these maps corresponds to 285 × 120 pc at the assumed distance of 15 Mpc. Plots of brightness vs. declination are shown in Fig. 4. The three maps are similar at each wavelength; the radio continuum emission comes from a compact strong source and an extension to the north. The peak position at each frequency differs by 2'' in R. A. from the optical position, but given the uncertainties in the optical position we assumed that the strongest radio emission originates from the optical nucleus. No radio emission is detected beyond a radius of 10'' from the nucleus to a level of 0.12 mJy beam^{−1} at 20 cm. The spectral indices of the nuclear source, ($S_\nu \propto \nu^\alpha$), from the integrated fluxes in Table 3 are $\alpha_{20}^0 \sim -0.52 \pm 0.02$; $\alpha_{20}^2 \sim -0.23 \pm 0.02$ and $\alpha_6^0 \sim +0.06 \pm 0.02$. The spectral indices of the northern source are $\alpha_{20}^0 \sim -0.20 \pm 0.05$; $\alpha_{20}^2 \sim +0.08 \pm 0.02$ and $\alpha_6^2 \sim +0.38 \pm 0.05$.

3. Millimeter observations and results

The CO(1–0) and CO(2–1) observations were made in November 1989 with the 15 m Swedish-ESO telescope (SEST) in La Silla, Chile. The half-power beamwidth was $\sim 44''$ at 115 GHz and $\sim 22''$ at 230 GHz. We used Schottky mixers with SSB receiver temperatures of 300 and 700 K for the 115 and 230 GHz lines respectively. The system temperatures outside the atmosphere were 450 and 1100 K respectively. The main beam efficiencies used to obtain T_{mb} were for 115 and 230 GHz lines, 0.68 and 0.51. The backend was an acousto-optic spectrometer with 728 channels each 690 kHz wide. The data were smoothed to a velocity resolution of 14.6 km s^{−1}. Velocities quoted here are heliocentric. We used a 6 Hz dual beam switching procedure with two symmetric reference positions offset by 12' in azimuth. We integrated typically one hour on each point. Pointing was checked at least every two hours by observations of radio sources, planets and SiO masers. The pointing errors were about 5'' rms.

The CO spectra (Fig. 5) show that the source is not resolved in the CO(1–0) line by the 44'' beam, while in the CO(2–1) line the

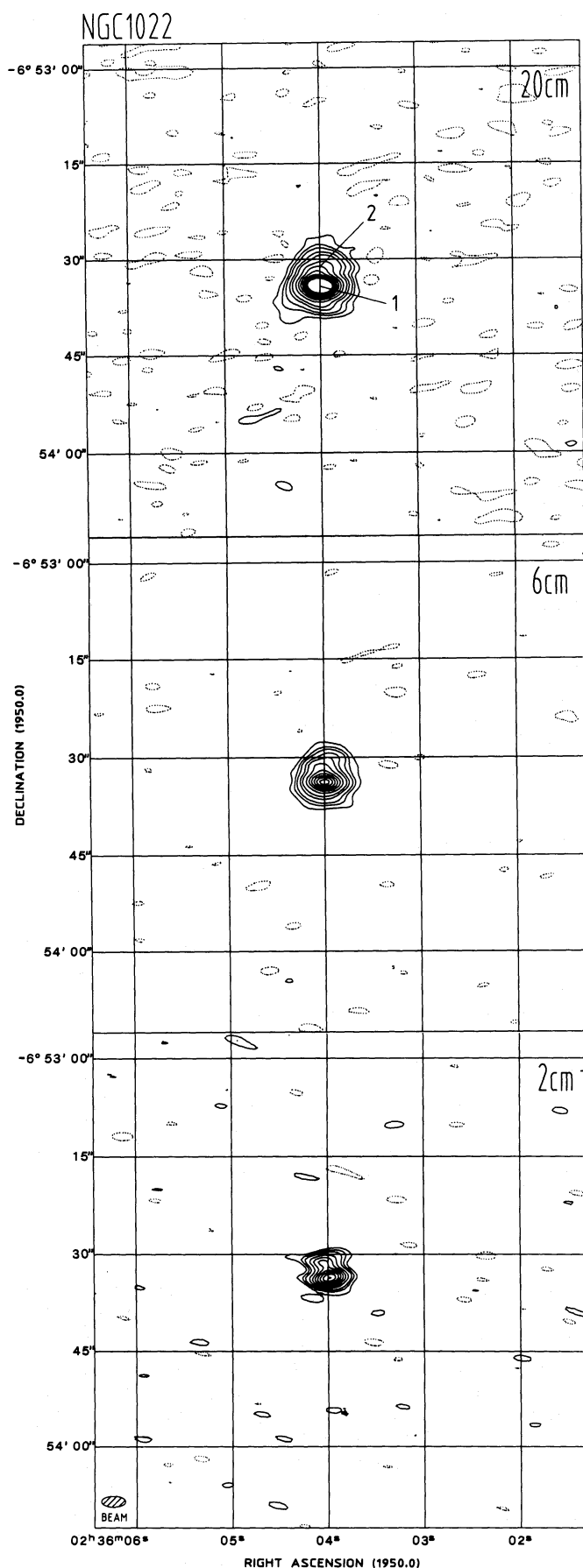


Fig. 2. High resolution radio continuum emission at 20 cm (above), 6 cm (middle) and 2 cm (bottom) from NGC 1022. The contour levels in each map are −0.12, 0.24, 0.48, 0.72, 1.2, 1.7, 2.6, 3.6, 4.6, 5.5, 6.5, 7.4, and 8.4 mJy beam^{−1}, except in the 2 cm map where the negative contour level is −0.72 mJy beam^{−1} and the first positive contour level is 0.72 mJy beam^{−1}.

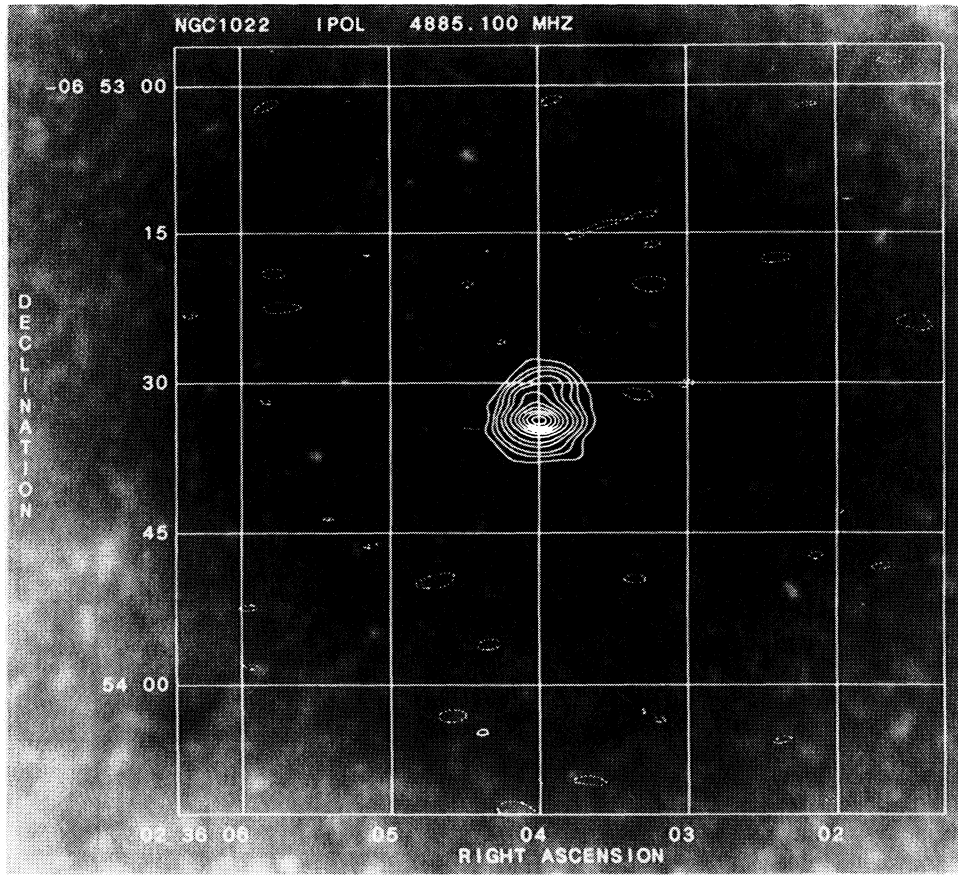


Fig. 3. High resolution map of the radio continuum emission at 6 cm from NGC 1022, superposed on a POSS blue sensitive photograph. Same contours as in Fig. 2

Table 3. Radio properties of NGC 1022

	$S_{1.4\text{GHz}}$ (mJy)	$S_{4.86\text{GHz}}$ (mJy)	$S_{14.9\text{GHz}}$ (mJy)
Total flux	43	—	—
Total central flux	39	20.7	22.3
Nuclear source peak	14.05	8.11	8.47
Integrated flux nuclear source	27.0 ^a	15.6	16.8
Northern source peak	3.65	2.86	4.45
Position of nuclear source	$\alpha(1950) = 02^{\text{h}}06^{\text{m}}03^{\text{s}}.86$ $\delta(1950) = -06^{\circ}53'34''$		

^a Integrated flux computed for a deconvolved source size of $2''.5 \times 2''.2$ at P.A. 153° .

beam-broadened width is $\simeq 28''$, compatible $17''$ source size. Since we barely resolved the source, and because of the low inclination of the galaxy on the sky, no rotation is evident from the spectra. The width of the average spectrum is the same as the central spectrum, $\Delta V_{\text{FWHM}} \simeq 120 \text{ km s}^{-1}$. This gives an order of magnitude of the maximum rotation velocity, in the range from ~ 130 to 150 km s^{-1} in the plane of the galaxy depending on the assumed inclination. There is no indirect evidence of a CO ring, in particular since the central spectrum does not present two velocity components. But this does not rule out the presence of a small ring, of radius smaller than the turn-over radius of the rotation curve. Our $22''$ beam is not sufficient to clarify this point.

The total mass of H_2 observed is $M(\text{H}_2) \simeq 1.2 \cdot 10^9 M_{\odot}$, with an adopted conversion ratio, $N(\text{H}_2)/I(\text{CO}) = 2.3 \cdot 10^{20} \text{ H}_2 \text{ molecules cm}^{-2}/\text{K km s}^{-1}$.

To get some insight in the CO lines' excitation, we convolved the CO(2–1) map to the $44''$ resolution. The superposition of the CO(1–0) and (2–1) spectra (Fig. 6) yields a ratio of integrated intensities $R(2-1)/R(1-0) \simeq 0.93 \pm 0.07$ which is compatible with a value of 1. In the disk of spiral galaxies, this ratio is near 0.5 (Braine et al. 1991), which implies subthermal excitation for the CO(2–1) line. A line ratio of 1 is the one expected from an optically thick gas, provided that the molecular density is high enough to excite both lines. The observed ratio of 1 in NGC 1022 which refers to a region of $44''$ or 3.3 kpc in diameter, means either that the emission is coming from dense clouds all over the region, or that a significant part of the emission is coming from a central zone, for which the ratio $R(2-1)/R(1-0)$ ratio is above 1. The requirements in NGC 1022 that the internal densities be high and that the line ratio is higher than 1 would lead to unusual properties for the molecular clouds there similar to the ones observed in M 82 (Knapp et al. 1980; Young & Scoville 1984). A possible scenario in NGC 1022 would be that the CO emission comes from a central region where there is currently a starburst activity as implied by the IRAS colors, namely the high dust temperature (see 5.3) and that the CO line ratio is indeed about 1. However, as mentioned by Young & Scoville (1984) a second interpretation would be that the clouds could be heated by an external radiation field, rather than by internal sources, raising the temperature on the outside of each cloud. The ratio $L_{\text{FIR}}/M(\text{H}_2) \simeq 4$ obtained here for NGC 1022 corresponds however to an almost normal star formation rate (Young et al. 1986).

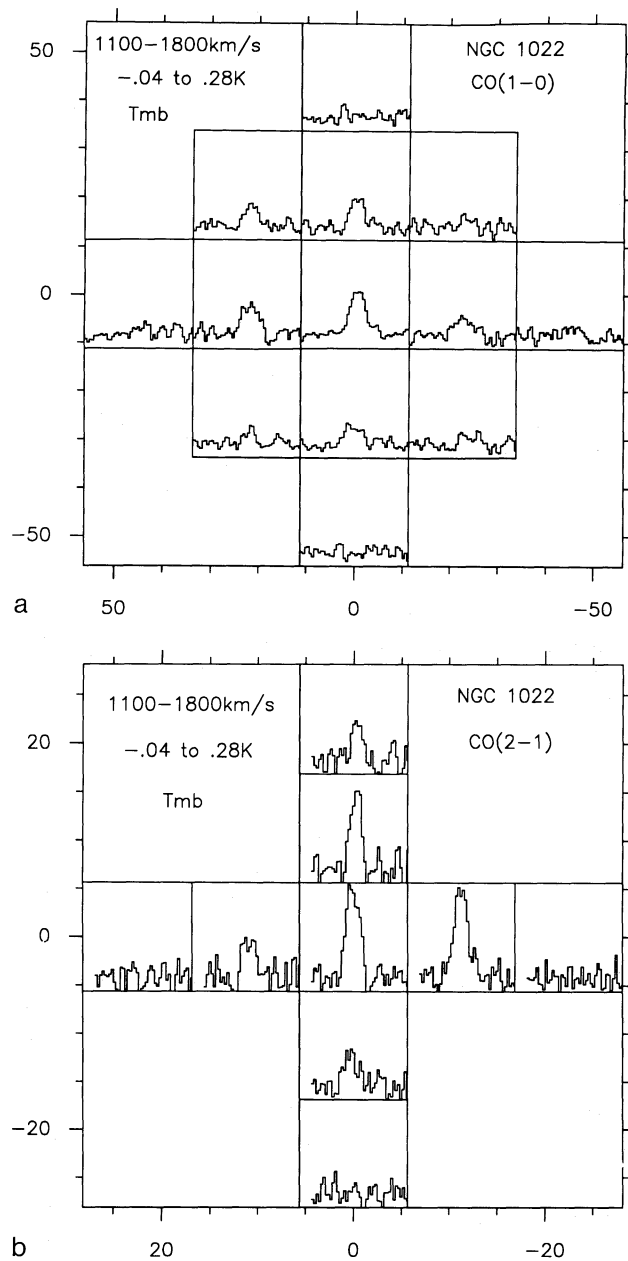
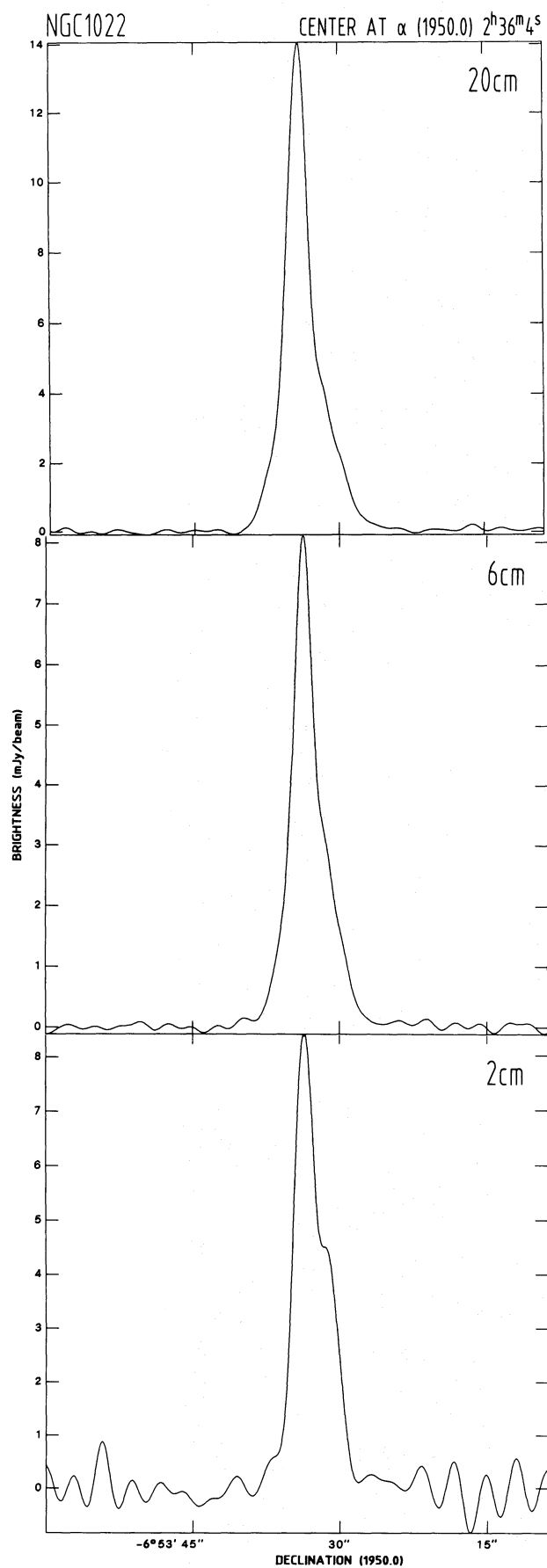


Fig. 5. a CO(1–0) and b CO(2–1) spectra obtained towards NGC 1022 with the SEST 15 m telescope. The velocity resolution is degraded to 14.6 km s^{-1} . The spatial resolutions are $44''$ and $22''$ respectively

Fig. 4. Radio continuum brightness distribution at 20 cm (above), 6 cm (middle) and 2 cm (bottom) versus declination, centered at $\alpha(1950) = 02^h36^m04^s$

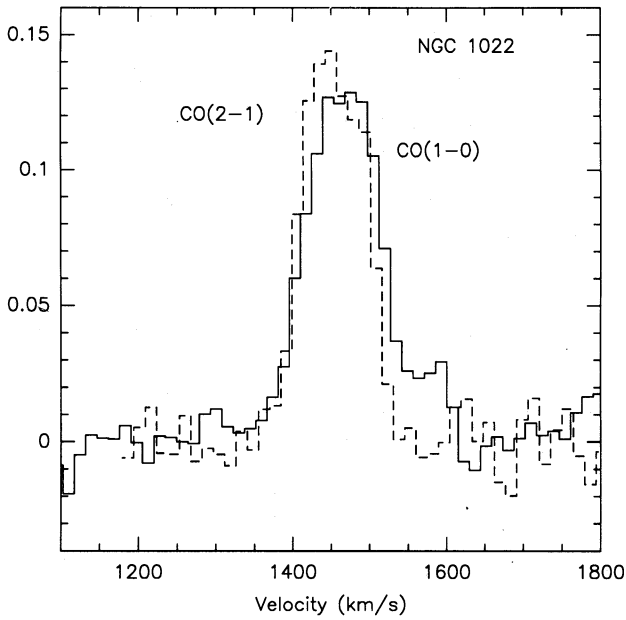


Fig. 6. Superposition of the convolved CO(2–1) spectrum with the CO(1–0) in the center, in the T_{mb} scale. The global ratio of integrated intensity $R(2-1)/R(1-0)$ is close to 1

4. Near-infrared observations and results

The near-IR observations were made with the 2.12 m telescope in San Pedro Martir, Baja California, Mexico in 1986. We used a single element InSb detector at J (1.2 μm), H (1.65 μm) and K (2.2 μm) bands at the $f/31$ Cassegrain focus (Roth et al. 1984). The aperture was 14", and the 10 Hz chopper throw was 100" in declination. The photometry was calibrated on SAO stars (Tapia et al. 1986). Several 5 s scans were taken at each wavelength at the position of the H -band peak. We then computed flux densities (Table 5) relative to a scale of 1520, 980, and 620 Jy at 1.2, 1.65, and 2.2 μm respectively for a zero-mag star (Beckwith et al. 1976). The observed near-IR colors, $J-H=0.82$ and $H-K=0.35$ are redder than the colors from normal spiral galaxies (Aaronson 1977; Carico et al. 1986) but similar to other barred spiral galaxies like NGC 1097 and NGC 613 which have circumnuclear star formation (Hummel et al. 1987a, b).

Our fluxes with a 14" aperture can be compared with the fluxes obtained with an aperture of 5"5 by Devereux et al. (1987) to determine the 2.2 μm curve of growth. If we assume that the 2.2 μm flux is a power law function of the aperture used ($F \propto a^\gamma$), then we obtain $\gamma \sim 0.87$, which agrees with the value of $\gamma \sim 0.83$ obtained by Devereux (1989) using fluxes with apertures of 3"6, 5"5, 7"2 and 9"3. Devereux et al. (1987) estimate the central mass of galaxies using velocity dispersions and multi-aperture 2.2 μm observations. In their calculation they assume that the 2.2 μm luminosity traces mass; that the M/L ratio is constant with radius,

Table 4. Thermal fluxes of NGC 1022

	Non-thermal spectral index (α)	Thermal flux (mJy)			$S_{\text{thermal}}/S_{\text{peak}}$ (%)		
		20 cm	6 cm	2 cm	20 cm	6 cm	2 cm
Nuclear source	–0.85	5.7	5.0	4.5	40	62	53
Northern source	–0.85	2.9	2.6	2.3	80	90	52
Nuclear source	–1.0	6.5	5.8	5.2	46	71	61
Northern source	–1.0	3.0	2.6	2.4	82	92	53
Total integrated flux	–0.85	20.7	11.0	11.8	53	53	53
	–0.85	15.6	12.8	11.8	40	62	63
Total integrated flux	–1.0	23.8	12.6	13.6	61	61	61
	–1.0	18.0	14.7	13.6	46	71	61

Table 5. Near-infrared photometry of NGC 1022

Filter band	Wavelength (μm)	Flux density ^a (mJy)				
		3"6	5"5	7"2	9"3	14"
J	1.25	–	20	–	–	52
H	1.65	19	29	–	46	70
K	2.2	18	27	34	39	61
N	10.0		374 \pm 23			
	10.0 ^b		160 \pm 40			

Estimated error 0.1 mag = 5 mJy.

^a Fluxes with 3"6, 5"5, 7"2 and 9"3 apertures are taken from Devereux et al. (1987) and Devereux (1989).

^b Pompea & Rieke (1989).

Table 6. Properties of NGC 1022

FIR luminosity	6.8 $10^9 L_\odot$
Lyman continuum photons	2 10^{53} s^{-1}
Blue luminosity ^a	7.4 $10^9 L_\odot$
Star formation rate	1.1 $M_\odot \text{ yr}^{-1}$
Molecular hydrogen mass	1.2 $10^9 M_\odot$
Atomic hydrogen mass ^b	< 2.2 $10^8 M_\odot$
Central gravitational mass	1.7 $10^9 M_\odot$
Ionized hydrogen mass	< 1.3 $10^7 M_\odot$
Dust temperature ^c	40 K

^a Tully (1988).

^b Huchtmeier (1982).

^c Assuming $S_\nu \sim \nu B_\nu(T)$.

and that the mass is spherically distributed in the inner regions. Because there is not yet a published value for the velocity dispersion in NGC 1022, no good estimate of the central mass can be given. Instead we attempt to estimate the central mass from the maximum rotational velocity observed in the CO spectrum of the central region obtained with a beamsize of $45''$. By doing this we are aware that the estimated central mass will certainly differ from the true central mass but this difference is not too large in terms of the assumptions made. Following Devereux et al. (1987) the central mass inside a radius r is $M_{\odot} (r \leq 200) = 233 \beta r_{\text{pc}} \sigma^2 M_{\odot}$, where for NGC 1022 $\beta = 2.15$. The reported values for the inclination of the galaxy are about similar, namely, $i \simeq 28^\circ$ (Tully 1988) and $i \simeq 24^\circ$ (Grosbol 1985) therefore the values used for σ would be $\sigma_1 = 130 \text{ km s}^{-1}$ and $\sigma_2 = 150 \text{ km s}^{-1}$ which are one half of the observed FWHM CO(1–0) line after correcting for the inclination. The estimated central mass would then be in the range from $1.7 \cdot 10^9 M_{\odot}$ to $2.25 \cdot 10^9 M_{\odot}$.

5. Discussion

5.1. Origin of the radio emission: star formation or active nucleus?

The total radio continuum emission at each frequency is assumed to be the sum of optically thin synchrotron emission, $S_{\text{NT}} \propto \nu^{\alpha}$, and an optically thin thermal emission, $S_{\text{TH}} \propto \nu^{-0.1}$. Since we mapped the emission at the three wavelengths with similar spatial resolution, we are able to calculate the relative amounts of thermal and non-thermal emission. In order to determine the thermal 2 cm emission, we need to know the non-thermal spectral index α and the total observed fluxes at 20 cm and 6 cm. We computed the thermal fluxes corresponding to two values of α , $\alpha = -0.85$ and $\alpha = -1$. The estimated thermal fluxes from the nuclear source (source 1 in Fig. 2) are listed in Table 4. The estimated thermal fluxes from the northern source are more uncertain because the source is less prominent and its existence is only hinted in the north-south brightness plot (see Figs. 3 and 4).

The peak non-thermal fluxes from the central nuclear source are 4.2 mJy at 2 cm, 3.4 mJy at 6 cm, and 8.75 mJy at 20 cm. The observed non-thermal spectral indices are $\alpha_{20}^{\text{nt}} \sim -0.80$, $\alpha_{20}^{\text{nt}} \sim -0.31$, and $\alpha_6^{\text{nt}} \sim +0.20$. These values of α_{20}^{nt} and α_6^{nt} imply that there is an excess of 2 cm emission suggesting thermal origin (H II regions). These regions are too large ($\geq 200 \text{ pc}$) to be opaque at 20 and 6 cm and therefore the possibility of having optically thick H II regions (which would mimic the derived spectral indices) is not favored. Another possibility, which we prefer to believe, is that the non-thermal spectral index is about or a little steeper than the value of -0.8 assumed here and that part or all of the 2 and 6 cm emission is from optically thin H II regions. A second possibility is that there is a contribution from a compact, non-thermal nuclear source which is synchrotron self absorbed similar to the nuclear source observed in the barred galaxy NGC 1097 (Hummel et al. 1987). The warm dust temperature; the detection of the $10 \mu\text{m}$ emission from the inner central regions; the detection and extent of the CO emission and the observed radio spectral indices suggest the existence of thermal emission from the central region of NGC 1022.

If the estimated thermal emission is correct, then the flux of the central source at 2 cm corresponds to $N_{\text{Ly}\alpha} \sim 2.01 \cdot 10^{53} \text{ s}^{-1}$ or approximately the number of Lyman continuum photons from $5 \cdot 10^4$ O7 ZAMS stars; an electron density, for a source size of $2''.5$, of 50 cm^{-3} ; an emission measure is $\int n_e^2 dV \sim 6.9 \cdot 10^5 \text{ pc cm}^{-6}$ and the ionized mass is $M_i \sim 1.3 \cdot 10^7 M_{\odot}$. The expected H α flux would

be $S_{\text{H}\alpha} \sim 10^{-11} \text{ erg cm}^{-2} \text{ s}^{-1}$. The observed H α flux is $S_{\text{H}\alpha}^{\text{observed}} \sim 7.2 \cdot 10^{-13} \text{ erg cm}^{-2} \text{ s}^{-1}$ (Kennicutt & Kent 1983), which would be consistent with the observed thermal radio flux if the average extinction were $A_{\text{H}\alpha} \simeq 3 \text{ mag}$.

In other barred galaxies as NGC 613, NGC 1097 (Hummel et al. 1987a, b), NGC 1326 and NGC 4314 (Garcia-Barreto et al. 1991a, b) the radio continuum comes from circumnuclear rings at distances from the nucleus expected for an inner Lindblad resonance, ILR, where the material piles up at the resonance thereby favoring the formation of stars, giant H II regions, warm dust, supernovae and hence, non-thermal radio radiation. In NGC 1022 there is no evidence from the radio continuum or from the CO of the existence of a ring structure unless its diameter is $\leq 11''$ or 800 pc (the size of the low level contours of the radio continuum emission, see Fig. 2). The spatial distribution of the radio continuum and the observed spectral indices do not exclude either the possibility of the presence of a compact source with an inverted spectrum such as observed in NGC 1097 (Hummel et al. 1987b).

5.2. Gas content in the central region

The $M(\text{H}_2)/L_B$ ratio is $\simeq 0.2$ which indicates that the H_2 content is relatively high for such an early-type galaxy (the average value for Sab galaxies it is 0.08, Young & Knezek 1989). In particular, since the atomic hydrogen, H I, is not detected (Huchtmeier 1982), and $M(\text{H I}) \leq 2.2 \cdot 10^8 M_{\odot}$, the ratio of molecular to atomic gas is $M(\text{H}_2)/M(\text{H I}) \geq 8$ well above the average value of 4 for S0-Sa galaxies and 2.2 for Sab galaxies (Young & Knezek 1989).

5.3. Far-infrared observations: star formation in the central region?

The fluxes from NGC 1022 detected by IRAS were $0.73 \pm 0.03 \text{ Jy}$ at $12 \mu\text{m}$, $3.37 \pm 0.04 \text{ Jy}$ at $25 \mu\text{m}$, $19.55 \pm 0.04 \text{ Jy}$ at $60 \mu\text{m}$ and $26.72 \pm 0.14 \text{ Jy}$ at $100 \mu\text{m}$ (Soifer et al. 1989). The FIR colors of NGC 1022 between 12 and $25 \mu\text{m}$, and between 60 and $100 \mu\text{m}$, are similar to the colors of other barred spiral galaxies with circumnuclear star formation such as NGC 613, NGC 1097 (Hummel et al. 1987a, b), NGC 1326 and NGC 4314 (Garcia-Barreto et al. 1991a, b). The characteristic dust temperature, 40 K, computed using the IRAS fluxes and a flux density proportional to the frequency times the black body curve, is however, about 20% higher than the characteristic dust temperature of other isolated galaxies ($\langle T_{\text{dust}} \rangle \sim 34 \text{ K}$, Solomon & Sage 1988) and is comparable to that found in interacting galaxies ($\langle T_{\text{dust}} \rangle \sim 41 \text{ K}$, Solomon & Sage 1988) and in other barred galaxies like NGC 1097. The FIR luminosity from NGC 1022 is $L_{\text{FIR}} = 6.8 \cdot 10^9 L_{\odot}$ and its blue luminosity is $L_B = 7.4 \cdot 10^9 L_{\odot}$ (Tully 1988). The formation rate of O, B, A stars is $\text{SFR} \sim 8 \cdot 10^{-11} L_{\text{TOT}}$ in $M_{\odot} \text{ yr}^{-1}$ (Scoville & Young 1983) which for NGC 1022 is then $\text{SFR} \sim 1.1 M_{\odot} \text{ yr}^{-1}$. This star formation rate is about 10 times higher than the mean star formation rate found in Virgo spirals (Scoville et al. 1983). More evidence for star formation in the central region of NGC 1022 is also provided by the $10 \mu\text{m}$ flux density of $S_{10\mu\text{m}} = 374 \pm 23 \text{ mJy}$ from an aperture of $5''.5$ (Devereux 1987) and $S_{10\mu\text{m}} = 160 \pm 40 \text{ mJy}$ from an aperture of $5''.5$ (Pompea & Rieke 1989). The theoretical ratio $S_{10\mu\text{m}}/S_{2\text{cm}}$ calculated for hot dust temperatures between $T_G = 200 \text{ K}$ and 400 K ranges from 14 to 33 (Genzel et al. 1982; Scoville et al. 1983). The expected 2 cm thermal emission from NGC 1022 from a region with radius $r \leq 2''.75$ with a ratio of 25 would be between 7 and 15 mJy , which is consistent with the observed fluxes from the central and the northern sources and thus strongly suggests massive stars as the

origin for the heating of the dust. The general properties of NGC 1022 are listed in Table 6.

6. Conclusions

IRAS observations of spiral galaxies indicate that galaxies with a bar have FIR colors characteristic of star formation activity in the vicinity of the compact nucleus and in some cases this is corroborated by the presence of a ring-like structure in the radio continuum emission, in H α and sometimes in the CO emission. In this paper we reported new observations of the barred spiral galaxy NGC 1022 in the radio continuum CO and NIR bands. Our observations support the idea that there is star formation activity in the vicinity of the nucleus but give no evidence of a ring like structure. Our main conclusions are: (a) the radio continuum emission is observed only from the nucleus with a weaker extension to the north. No radio continuum emission is observed beyond the inner 20". (b) From multi-aperture 2.2 μ m observations we estimate a central mass of about $2 \cdot 10^9 M_{\odot}$. (c) We determine a molecular mass $M(H_2) \simeq 1.2 \cdot 10^9 M_{\odot}$. The molecular to atomic mass ratio is $\simeq 8$.

Acknowledgements. We thank the staff of the VLA and San Pedro Martir, México for their help during the observations and G. Hutschenreiter and W. Fusshöller for their photographic work and preparation of the figures. The VLA is a facility of the National Radio Astronomy Observatory and is operated by Associated Universities under contract with the U.S. National Science Foundation. It is a pleasure to thank the referee, Dr. T. van der Hulst for his valuable comments and suggestions that helped us to improve this paper. JAG-B acknowledges partial financial support from CICB-UAEM (Toluca, Mexico), CONACYT (Mexico) grant PCCBBNA-022688 and a Junior Fellowship from the Alexander von Humboldt-Stiftung, Federal Republic of Germany.

References

- Aaronson M., 1977, Ph. D. thesis, Harvard University
 Braine J., Combes F., Casoli F., et al., 1991, A&A (in press)
 Carico D. P., Soifer B. T., Beichman C., Elias J. H., Matthews K., Neugebauer G., 1986, AJ 92, 1254
 Condon J. J., 1987, ApJS 65, 485
 Combes F., 1988, in: Galactic and Extragalactic Star Formation. Pudritz R. E., Fich M. (eds.) Kluwer, Dordrecht, p. 475
 Combes F., Gerin M., 1985, A&A 150, 327
 Devereux N. A., Becklin E. E., Scoville N., 1987, ApJ 312, 529
 Devereux N. A., 1987, ApJ 323, 91
 Devereux N. A., 1989, ApJ 346, 126
 Fisher J. R., Tully R. B., 1981, ApJS 47, 139
 Garcia-Barreto J. A., Dettmar R.-J., Combes F., Gerin M., Koribalski B., 1991a, Rev. Mex. Astron. Astrofis. (in press)
 Garcia-Barreto J. A., Downes D., Combes F., Gerin M., Magri C., Carrasco L., Cruz-Gonzalez I., 1991b, A&A 244, 257
 Genzel R., Becklin E. E., Wynn-Williams C. G., Moran J. M., Reid M. J., Jaffe D. T., Downes D., 1982, ApJ 255, 527
 Giogia I. M., Gregorini L., Klein U., 1982, A&A 116, 164
 Grosbol P. J., 1985, A&AS 60, 261
 Griesmith D., 1980, AJ 85, 789
 Hawarden T. G., Mountain C. M., Leggett S. K., Puxley P. J., 1986, MNRAS 221, 41p
 Huchtmeier W. K., 1982, A&A 110, 121
 Hummel E., van der Hulst J. M., Keel W. C., 1987a, A&A 172, 51
 Hummel E., Jörsäter S., Lindblad P. O., Sandqvist A., 1987b, A&A 172, 32
 Hummel E., van der Hulst J. M., Kennicutt R. C., Keel W. C., 1990, A&A 236, 333
 Kennicutt R. C., Kent S. M., 1983, AJ 88, 1094
 Knapp G. C., Phillips T. G., Huggins P. J., Leighton R. B., Wannier P. G., 1980, ApJ 240, 60
 Norris R. P., Gardner F. F., Whiteoak J. B., Allen D. A., Roche P. F., 1989, MNRAS 237, 673
 Pompea S. M., Rieke G. H., 1989, ApJ 342, 250
 Puxley P. J., Hawarden T. G., Mountain C. M., 1988, MNRAS 231, 465
 Roth M., Iriarte A., Tapia M., Resendiz G., 1984, Rev. Mex. Astron. Astrofis. 9, 25
 Schwartz M. P., 1981, ApJ 247, 77
 Schwartz M. P., 1984, MNRAS 209, 93
 Scoville N. Z., Young J. S., 1983, ApJ 265, 148
 Scoville N. Z., Becklin E. E., Young J., Capps R. W., 1983, ApJ 271, 512
 Soifer B. T., Boehmer L., Neugebauer G., Sanders D. B., 1989, AJ 98, 766
 Solomon P. M., Sage L. J., 1988, ApJ 334, 613
 Tapia M., Neri L., Roth M., 1986, Rev. Mex. Astron. Astrofis. 13, 115
 Tully R. B., 1988, Nearby Galaxies Catalog. Cambridge Univ. Press, Cambridge, p. 201
 Young J. S., Knezek P. M., 1989, ApJ 347, L55
 Young J. S., Schloerb F. P., Kenney J. D., Lord S. D., 1986, ApJ 304, 443
 Young J. S., Scoville N. Z., 1984, ApJ 287, 153